

Bi-relaxation behaviors in epitaxial multiferroic double-perovskite $\text{BiFe}_{0.5}\text{Mn}_{0.5}\text{O}_3/\text{CaRuO}_3$ heterostructures

J. Miao, X. Zhang, Q. Zhan, Y. Jiang, and K.-H. Chew

Citation: *Appl. Phys. Lett.* **99**, 062905 (2011); doi: 10.1063/1.3624847

View online: <http://dx.doi.org/10.1063/1.3624847>

View Table of Contents: <http://apl.aip.org/resource/1/APPLAB/v99/i6>

Published by the AIP Publishing LLC.

Additional information on *Appl. Phys. Lett.*

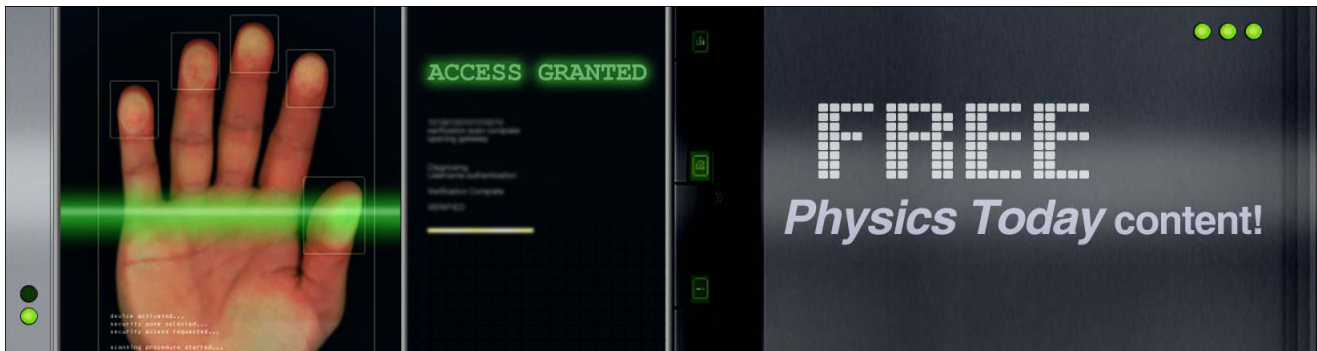
Journal Homepage: <http://apl.aip.org/>

Journal Information: http://apl.aip.org/about/about_the_journal

Top downloads: http://apl.aip.org/features/most_downloaded

Information for Authors: <http://apl.aip.org/authors>

ADVERTISEMENT



Bi-relaxation behaviors in epitaxial multiferroic double-perovskite $\text{BiFe}_{0.5}\text{Mn}_{0.5}\text{O}_3/\text{CaRuO}_3$ heterostructures

J. Miao,^{1,a)} X. Zhang,¹ Q. Zhan,¹ Y. Jiang,^{1,b)} and K.-H. Chew²

¹State Key Laboratory for Advanced Metals and Materials, School of Materials Science and Engineering, University of Science and Technology Beijing, Beijing 100083, China

²Department of Physics, University of Malaya, 50603 Kuala Lumpur, Malaysia

(Received 9 June 2011; accepted 22 July 2011; published online 12 August 2011)

Multiferroic double-perovskite $\text{BiFe}_{0.5}\text{Mn}_{0.5}\text{O}_3$ thin film heterostructures were epitaxially grown on CaRuO_3 -buffered (001) SrTiO_3 by pulse laser deposition. Typical Vogel-Fulcher relaxorlike dielectric and magnetic susceptibilities were observed, implying the film exhibits the properties of an electric relaxor and a magnetic relaxor. Polarization and size of polar nanoregions (PNRs) were determined by fitting the dielectric constant to a multi-polarization mechanism model. It was found that PNRs of 7-11 nm decrease from $0.67 \mu\text{C}/\text{cm}^2$ to $0.11 \mu\text{C}/\text{cm}^2$, as the temperature increases from 380 K to 460 K. A weak ferromagnetism was observed via magnetic hysteresis loops up to 300 K. © 2011 American Institute of Physics. [doi:10.1063/1.3624847]

Multiferroic materials, such as BiFeO_3 (Ref. 1) and BiMnO_3 ,² suffer from the drawbacks of a high leakage current at room temperature or a low temperature for the appearance of multiferroic properties. Recently, multiferroics with double-perovskite structures $\text{Bi}_2(\text{B}'\text{B}'')\text{O}_6$ (where B' has partially filled e_g -orbitals and B'' has empty e_g -orbitals, or vice versa) were identified as a potential candidate that may provide a unique opportunity to promote multiferroic behaviors.³ Some of candidates have been investigated, such as $\text{Bi}_2\text{FeCrO}_6$ (Ref. 4) and $\text{Bi}_2\text{NiMnO}_6$.⁵ However, few researchers have focused on the multiferroic double perovskite $\text{Bi}_2\text{FeMnO}_6$ (BFMO).⁶⁻¹⁰

Other interesting properties that could be anticipated from these double-perovskite multiferroics are the relaxor behaviors due to its B -site fluctuation in $\text{Bi}_2(\text{B}'\text{B}'')\text{O}_6$ structure. Relaxor behaviors are normally associated with the existence of polar nanoregions (PNRs) as a result of nanoscale compositional inhomogeneities.¹¹ Typical ferroelectrics such as $\text{Pb}(\text{Mg}_{1/3}\text{Nb}_{2/3})\text{O}_3$,¹¹ $\text{BaZr}_{0.6}\text{Ti}_{0.4}\text{O}_3$,¹² and $\text{K}_{1/2}\text{Na}_{1/2}\text{NbO}_3$,¹³ were investigated as relaxors. On the other hand, some multiferroics $\text{Pb}(\text{Fe}_{1/2}\text{Nb}_{1/2})\text{O}_3$,¹⁴ $0.8\text{Pb}(\text{Fe}_{2/3}\text{W}_{1/3})\text{O}_3-0.2\text{PbTiO}_3$,¹⁵ and $0.8\text{Pb}(\text{Fe}_{1/2}\text{Nb}_{1/2})\text{O}_3-0.2\text{Pb}(\text{Mg}_{1/2}\text{W}_{1/2})\text{O}_3$ (Refs. 16 and 17) also exhibit relaxor behaviors.

While numerous works of double-perovskite multiferroics have been made on BFMO films,⁶⁻¹⁰ most of the studies were mainly focused on the magnetic properties of BFMO films. Very little work to date has been done on electric properties of BFMO films. In this study, the structural, electric, and magnetic properties of BFMO films epitaxially grown $\text{CaRuO}_3/\text{SrTiO}_3$ (CRO/STO) substrates were investigated. Interestingly, we found that the BFMO films exhibit not only the properties of an electric relaxor but also those of a magnetic relaxor, to be referred to as *birelaxor*.

Stoichiometric $\text{Bi}_{2.2}\text{FeMnO}_6$ ceramic target was prepared using a conventional solid reaction. A XeCl excimer laser (Compex205, $\lambda = 308 \text{ nm}$) of $1.5 \text{ J}/\text{cm}^2$ and 2 Hz was

used to fabricate the films. The BFMO film was deposited on a CRO layer at temperature $650-730^\circ\text{C}$ under 0.4 mbar oxygen pressure. After the fabrication, the heterostructures were *in-situ* annealed for 25 min at an oxygen pressure of 0.8 mbar and then cooled down to room temperature. The thicknesses of the BFMO and CRO layers were about 180 and 60 nm, respectively. For the electrical characterization, 200 nm Pt upper electrodes were deposited using magnetron sputtering through a metal shadow mask.

The phase identification was performed by a Philips X'Pert high resolution diffractometer. Dielectric properties of the BFMO/CRO heterostructures were measured using a HP4284a precision LCR meter. Polarization-voltage hysteresis loops were recorded using an aixACCT TF analyzer 2000. The temperature of the samples was stabilized using a CryoLab202 continuous-flow cryostat in the range from 150 K to 500 K. Magnetic properties were measured using a QD-MPMSXL5 superconducting quantum interference device magnetometer.

Figure 1(a) shows a θ - 2θ XRD linear scan of BFMO/CRO heterostructures on (001) STO crystal using $\text{CuK}\alpha_1$ ($\lambda = 1.5406 \text{ \AA}$) radiation. Only the ($h00$) BFMO and ($00l$) CRO reflections were observed, indicating the epitaxial growth of BFMO and CRO layers with the c -axes perpendicular to the STO substrate surface. The out-of-plane lattice parameter of BFMO film was estimated to be 3.952 \AA from its ($h00$) reflections ($2d\sin\theta = \lambda$). Figure 1(b) illustrates the φ -scans XRD of (202) BFMO, (202) CRO, and (202) STO reflections, respectively. Each layer shows an azimuthal diffraction pattern without other peaks at the intervals between four peaks. Accordingly, the fourfold symmetry in the φ -scans reveals an epitaxial nature of BFMO and CRO layers on STO substrate.

Figure 2(a) illustrates the temperature dependence of the dielectric permittivity ϵ_r' and dielectric loss $\text{tg}\delta$ in BFMO thin film. A frequency dispersion of ϵ_r' and peak temperature T_m were found around 400 K, indicating a dielectric relaxor behavior in the heterostructures. The dynamics of relaxor with PNRs can be characterized using the well-known Vogel-Fulcher (VF) relation¹⁸

^{a)}Author to whom correspondence should be addressed. Electronic mail: j.miao@ustb.edu.cn.

^{b)}Electronic mail: yjiang@ustb.edu.cn.

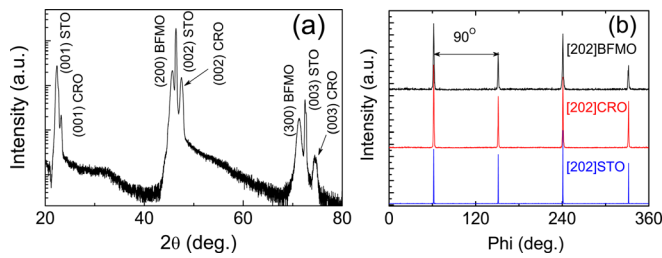


FIG. 1. (Color online) (a) X-ray θ - θ scan of a BFMO film deposited on (001)-oriented CRO/STO substrate; (b) the ϕ -scans XRD of (202) BFMO, (202) CRO, and (202) STO reflections, respectively.

$$\omega^{FE} = \omega_0^{FE} \exp[-E_a^{FE}/k_B(T_m - T_{VF}^{FE})], \quad (1)$$

where $\omega_0^{FE} = 2\pi f_0^{FE}$ denotes the characteristic relaxation frequency, E_a^{FE} the activation energy, k_B the Boltzmann constant, and T_{VF}^{FE} the VF freezing temperature. A good fitting with Eq. (1) between $\ln(\omega^{FE})$ and $1/T_m$ was found in the frequency range of 1 kHz–1 MHz, suggesting a VF-type dielectric relaxation in the film [inset of Fig. 2(a)]. Since the relationship of $\ln(\omega^{FE}) \propto 1/T_m$ is nonlinear, the Arrhenius-type relaxation process can be ruled out. Accordingly, E_a^{FE} and ω_0^{FE} were estimated to be 0.07 eV and 6.1×10^8 Hz, respectively, and T_{VF}^{FE} was extracted as 314 (± 3) K. Those obtained parameters are in good agreement with other multiferroic relaxors, such as $\text{Pb}(\text{Fe}_{0.66}\text{W}_{0.33})_{0.8}\text{Ti}_{0.2}\text{O}_3$ film¹⁵ ($E_a \sim 0.06$ eV; $\omega_0 \sim 1.7 \times 10^8$ Hz) and $\text{Pb}(\text{Fe}_{0.5}\text{Nb}_{0.5})_{0.8}(\text{Mg}_{0.5}\text{W}_{0.5})_{0.2}\text{O}_3$ film¹⁶ ($E_a \sim 0.06$ eV; $\omega_0 \sim 2.8 \times 10^8$ Hz).

In Fig. 2(b), we show the temperature dependence of macroscopic P – E hysteresis loops in BFMO films measured at 1 kHz. At temperature 350 K, an ellipselike shape was observed due to the considerable leakage currents at $T \sim T_m$. It can be seen that the lossy P – E loop gradually transforms to a well defined and saturated loop with decreasing temperature. Note that the remnant polarization (P_r) and coercive field (E_c) at $T < 250$ K were measured at $\sim 23 \mu\text{C}/\text{cm}^2$ and ~ 143 kV/cm, respectively. Those obtained values are considerably lower than that of $\text{Nd}:\text{BiFeO}_3/\text{Bi}_2\text{FeMnO}_6$ bilayer ($54 \mu\text{C}/\text{cm}^2$, 237 kV/cm) due to the presence of $\text{Nd}:\text{BiFeO}_3$ layer in the bilayer.⁸

In order to gain further insight on the presence of local PNRs in BFMO films, we examine the electric-field dependence of the dielectric constant $\epsilon_r(E)$ using the Landau-Devonshire theory by incorporating the cluster polarization contribution due to the reorientation of random-field-induced PNRs.¹⁹ Based on the model, the relation of $\epsilon_r(E)$ versus E is given by

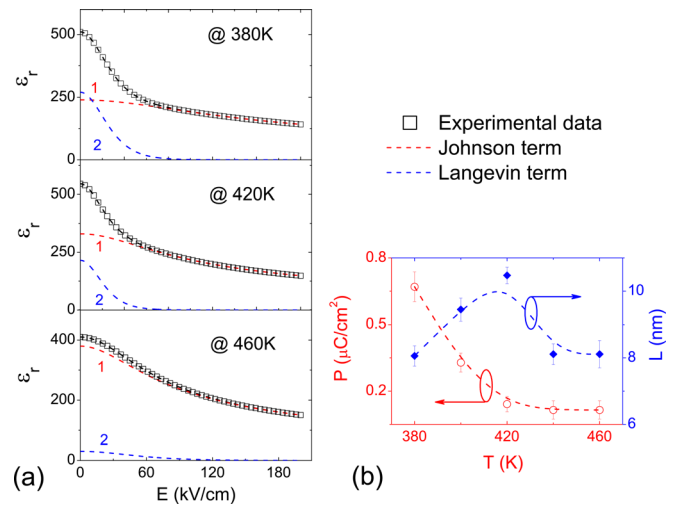


FIG. 3. (Color online) (a) dc electric-field dependence of ϵ_r at 10 kHz and several typical temperatures. Curve 1 is the contribution from the conventional polarizations and curve 2 from the PNRs; (b) temperature dependence of the polarization and dimension of the PNRs.

$$\epsilon_r(E) = \epsilon_r(0)/\{1 + \alpha[\epsilon_0\epsilon_r(0)]^3 E^2\}^{1/3} + P_0 x/\epsilon_0[\cosh(Ex)]^2, \quad (2)$$

where $x = P_0 L^3/(2k_B T)$ with the cluster polarization P_0 and dimension L , $\epsilon_r(0)$ and ϵ_0 are the dielectric permittivity at zero field and that of vacuum, and α is a parameter associated with anharmonic contributions. The first term on the right-hand of Eq. (2) is the Johnson relationship from Landau-Devonshire theory, describing the typical dielectric behaviors in paraelectric phase. The second term on the right-hand of Eq. (2) corresponds to the contributions from the Langevin-type re-orientational polar clusters. In Fig. 3(a), the $\epsilon_r(E)$ curves were fitted at three typical temperatures, 380 K, 420 K, and 460 K. It was found that the contributions of PNRs to the total dielectric permittivity at zero fields are 48.1%, 32.4%, and 7.4%, respectively. Figure 3(b) shows the fitting parameters of polarization and size of the PNRs as a function of temperature using the multi-polarization mechanism model. The result reveals that the polarization of PNRs decreases from $0.67 \mu\text{C}/\text{cm}^2$ to $0.11 \mu\text{C}/\text{cm}^2$ with increasing the temperature from 380 K to 460 K. The result is comparable with the values of 0–0.80 $\mu\text{C}/\text{cm}^2$ in $\text{Sr}_{0.997}\text{Bi}_{0.002}\text{TiO}_3$ ceramics¹⁹ and 0.1–0.4 $\mu\text{C}/\text{cm}^2$ in $\text{Sr}_{0.98}\text{Mn}_{0.02}\text{TiO}_3$ ceramics.²⁰ The dimension of PNRs is found to be within nanometer scale, $L = 7$ –11 nm. This value is also reasonable to that of 4–7.5 nm in $\text{Sr}_{0.997}\text{Bi}_{0.002}\text{TiO}_3$ ceramics¹⁹ and 7–12 nm in $\text{Sr}_{0.98}\text{Mn}_{0.02}\text{TiO}_3$

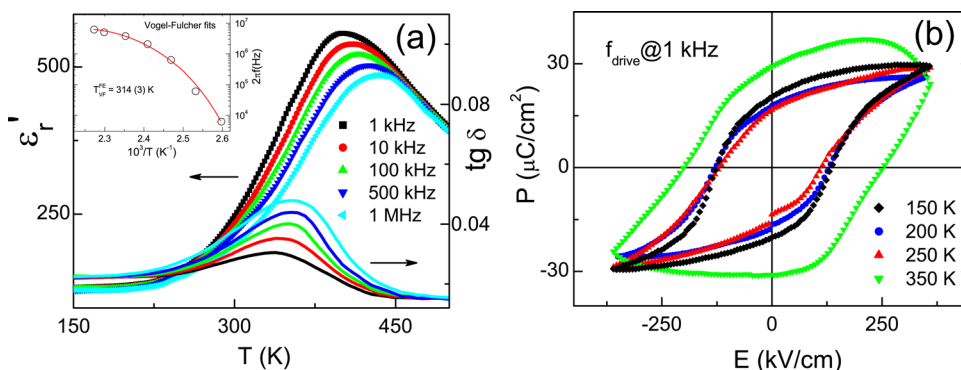


FIG. 2. (Color online) (a) Temperature dependence of the dielectric permittivity and loss in BFMO film from 1 kHz–1 MHz. (Inset) V-F behavior of the relaxation frequency; (b) macroscopic P - E loops at various temperatures.

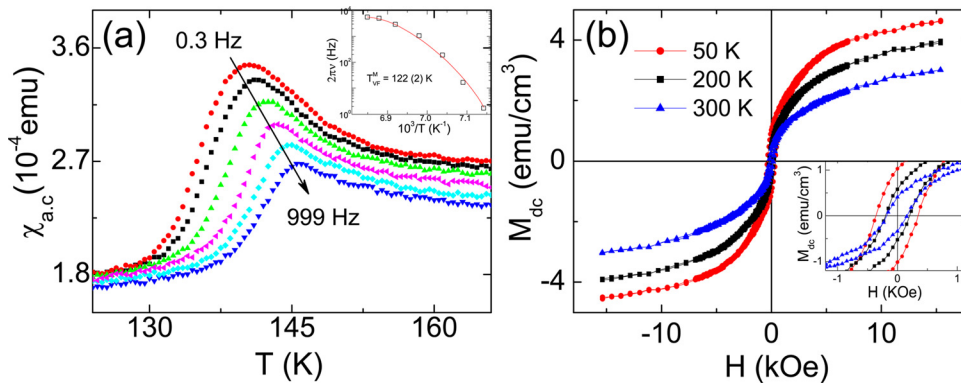


FIG. 4. (Color online) (a) Temperature dependence of the ac magnetic susceptibility at various frequencies. (Inset) V-F behavior of the effective relaxation frequency; (b) magnetic field dependence of the magnetization. (Inset) The magnified central region of the hysteresis loops.

ceramics.²⁰ Here, the origin of PNRs in the BFMO film can be attributed to following reasons: (i) the nanoscale compositional inhomogeneities induced by the B-site compositional substitution between $\text{Fe}^{3+}/\text{Mn}^{3+}$ in BFMO films result in local PNRs with a lower symmetry;²¹ (ii) the presence of artificial defects (such as oxygen vacancies or Bi vacancies), impurities, and inhomogeneous strains generated in BFMO films may be another origin of the PNRs.²²

Figure 4(a) shows a strong frequency dispersion in the real part of ac magnetic susceptibilities in BFMO film [$\chi_{ac}(f) \sim T$], suggesting a slow magnetic dynamic relaxation process.²³ The magnetic relaxation frequency ω_0^M and the VF freezing temperature T_{VF}^M can be obtained from

$$\omega_0^M = \omega_0^M \exp[-E_a^M/k_B(T_m - T_{VF}^M)], \quad (3)$$

where $\omega_0^M = 2\pi f_0^M$. From Eq. (3), ω_0^M and T_{VF}^M in BFMO film were estimated to be $1.8 \times 10^{14} \text{ s}^{-1}$ and $122 (\pm 2) \text{ K}$, respectively. Note here that the predicted ω_0^M value is significantly higher than that of ω_0^{FE} . This is expected due to the fact that electron dynamics is involved in T_{VF}^M , whereas T_{VF}^{FE} involves both the ion displacements and orderings.¹⁷ Thus, we can confirm that the BFMO film exhibits not only an electric relaxor feature, but also a magnetic relaxor behavior.

Figure 4(b) shows the magnetic field (H) dependence of the in-plane magnetization (M) between 50 and 300 K. A slim and unsaturated $M \sim H$ hysteresis loop with $M_r \sim 1 \text{ emu/cm}^3$ and $H_c \sim 310 \text{ Oe}$ was observed at 50 K, similar to the reported value in BFMO/Si films (330 Oe, 5 K).⁷ Thus, the observation further supports the Fe-O-Mn ferrimagnetic transition at $\sim 140 \text{ K}$. Above T_{VF}^M , the remnant magnetization M_r and coercivity H_c decrease with increasing temperature. The magnetic hysteresis loops was found to retain in the M - H curve up to 300 K. We believe that the magnetic hysteresis loops at 200 K and 300 K are closely related to the Mn-O-Mn antiferromagnetic ordering.⁷ This is because the magnetization and coercive fields of the two loops exhibit nearly the same.

In summary, an epitaxial single-phase BFMO film was grown on (001) CRO/STO by pulse laser deposition (PLD). A VF relationship is used to describe the dispersions of the dielectric and magnetic susceptibilities in BFMO films. It is found that PNRs dynamics is involved at T_{VF}^{FE} , whereas the electron dynamics is involved at T_{VF}^M . The “weak magnetisms” in BFMO film may be attributed to the ferrimagnetic arranged spins between Fe and Mn ions at $\sim 140 \text{ K}$, and the canted antiferromagnetic (AFM) arranged spins between Mn ions above 200 K. The observed frequency dependence of dielectric and

magnetic susceptibilities and multiferroic (electric and magnetic) behaviors further provide the evidence for the magneto-electric *bi*-relaxation nature in BFMO films.

This work was partially supported by the NSFC (Nos. 50802007, 50831002, and 51071022), the Key grant Project of the Chinese Ministry of Education (No. 309006), the National Basic Research Program of China (No. 2007CB936202), the Fundamental Research Funds for the Central Universities, and Fok Ying-Tong Education Foundation (No. 121046).

- ¹J. Wang, J. B. Neaton, H. Zheng, V. Nagarajan, B. Ogale, B. Liu, D. Viehland, V. Vaithyanathan, D. G. Schlom, U. V. Waghmare, N. A. Spaldin, K. M. Rabe, M. Wuttig, and R. Ramesh, *Science* **299**, 1719 (2003).
- ²M. Gajek, M. Bibes, A. Barthélemy, K. Bouzehouane, S. Fusil, M. Varela, J. Fontcuberta, and A. Fert, *Phys. Rev. B* **72**, 020406(R) (2005).
- ³P. Padhan, H. Z. Guo, P. LeClair, and A. Gupta, *Appl. Phys. Lett.* **92**, 022909 (2008).
- ⁴R. Nechache, C. Harnage, A. Pignolet, F. Normandin, T. Veres, L. Carignan, and D. Ménard, *Appl. Phys. Lett.* **89**, 102902 (2006).
- ⁵M. N. Iliiev, P. Padhan, and A. Gupta, *Phys. Rev. B* **77**, 172303 (2008).
- ⁶L. Bi, A. R. Taussig, H. Kim, L. Wang, G. F. Dionne, D. Bono, K. Persson, G. D. Ceder, and C. A. Ross, *Phys. Rev. B* **78**, 104106 (2008).
- ⁷Y. Du, Z. X. Cheng, S. X. Dou, X. L. Wang, H. Y. Zhao, and H. Kimura, *Appl. Phys. Lett.* **97**, 122502 (2010).
- ⁸H. Zhao, H. Kimura, Z. Cheng, X. Wang, and T. Nishida, *Appl. Phys. Lett.* **95**, 232904 (2009).
- ⁹P. Mandal, A. Sundaresan, C. N. R. Rao, A. Iyo, P. M. Shirage, Y. Tanaka, Ch. Simon, V. Pralong, O. I. Lebedev, V. Caignaert, and B. Raveau, *Phys. Rev. B* **82**, 100416 (2010).
- ¹⁰E. M. Choi, S. Patnaik, E. Weal, S.-L. Sahonta, H. Wang, Z. Bi, J. Xiong, M. G. Blamire, Q. X. Jia, and J. L. MacManus-Driscoll, *Appl. Phys. Lett.* **98**, 012509 (2011).
- ¹¹A. A. Bokov and Z.-G. Ye, *Phys. Rev. B* **74**, 132102 (2006).
- ¹²A. Dixit, S. B. Majumder, R. S. Katiyar, and A. S. Bhalla, *Appl. Phys. Lett.* **82**, 2679 (2003).
- ¹³J. Miao, X. G. Xu, Y. Jiang, and B. R. Zhao, *Appl. Phys. Lett.* **95**, 132905 (2009).
- ¹⁴L. Yan, J. F. Li, C. Suchicital, and D. Viehland, *Appl. Phys. Lett.* **89**, 132913 (2006).
- ¹⁵Ashok Kumar, I. Rivera, R. S. Katiyar, and J. F. Scott, *Appl. Phys. Lett.* **92**, 132913 (2008).
- ¹⁶W. Peng, N. Lemée, J.-L. Dellis, V. V. Shvartsman, P. Borisov, W. Kleemann, Z. Trontelj, J. Holc, M. Kosec, R. Blinc, and M. G. Karkut, *Appl. Phys. Lett.* **95**, 132507 (2009).
- ¹⁷A. Levstik, V. Bobnar, C. Filipič, J. Holc, M. Kosec, R. Blinc, Z. Trontelj, and Z. Jagličič, *Appl. Phys. Lett.* **91**, 012905 (2007).
- ¹⁸R. Pirc and R. Blinc, *Phys. Rev. B* **76**, 020101 (2007).
- ¹⁹A. Chen and Y. Zhi, *Phys. Rev. B* **69**, 174109 (2004).
- ²⁰A. Tkach, P.M. Vilarinho, and A.L. Kholkin, *J. Appl. Phys.* **101**, 084110 (2007).
- ²¹G. Y. Xu, Z. Zhong, Y. Bing, Z. G. Ye, and G. Shirane, *Nat. Mater.* **5**, 134 (2006).
- ²²D. A. Tenne, A. Soukiassian, M. H. Zhu, A. M. Clark, X. X. Xi, H. Choo-suwan, Q. He, R. Guo, and A. S. Bhalla, *Phys. Rev. B* **67**, 012302 (2003).
- ²³V. V. Shvartsman, S. Bedanta, P. Borisov, W. Kleemann, A. Tkach, and P. M. Vilarinho, *Phys. Rev. Lett.* **101**, 165704 (2008).